Volume 1 | Number 1 | Jan 2013 | Pages 1–100

Journal of
Materials Chemistry A

Materials for energy and sustainability
www.rsc.org/materialsA

Li⁺

ROYAL SOCIETY
OF CHEMISTRY

ROYAL SOCIETY
OF CHEMISTRY

www.rsc.org/materialsA

ARTICLE

Heavy Metal Sorption Properties of Magnesium Titanate Mesoporous Nanorods

Xueyun Wang,[ab] Jianhua Cai,[ab] Yanjun Zhang,[a] Lihua Li,[a] Li Jiang,[*a] and Chunru Wang[*a]

The effects of the chemical composition on properties, such as morphology, surface area, crystallinity and crystal structure of the magnesium titanate nanorods have been investigated. The adsorption performance of the magnesium titanate nanorods with changed chemical compositions presented significant difference. The amorphous sample Ti/Mg-1/5-500 with the highest surface area of 152 $m^2 \cdot g^{-1}$ possessed the largest Pb^{2+} adsorption capacity of 241 $mg \cdot g^{-1}$.

[10] ## Introduction

In the last decades environmental contaminations have become a serious problem around the world, especially in developing countries such as China, India, Bangladesh *etc.*. For example, some areas in Hunan and Guangxi provinces of China are [15] suffering from the drinking water pollution by heavy metals e.g. Pb(II), Cd(II) and Hg(II) *etc.* due to the insufficient treated industrial residues.[1-4] It is well known that the heavy metals are extremely dangerous to our health and environment, therefore, it is of vital importance to develop applied technologies to remove [20] heavy metals from the polluted drinking water.

Among all the water treatment methods including flocculation, adsorption, membrane separation and ion exchange, the adsorption technique is the most popular way to remove heavy metal contaminants from water because of its high efficiency, low [25] cost and high specific to heavy metal ions.[5-14] In general, the efficiency of heavy metal adsorption is associated with the surface area of an adsorbent. Nanomaterials possessing large surface areas and porous structures such as metal oxides,[15, 16] metal silicates,[17, 18] and ferrites *etc*.[9] have been widely used for [30] pollutant adsorption for their facile mass transportation and abundant active adsorption sites. Additionally, properties of the materials which can be altered by varying their chemical composition will affect the material performance in applications. Composite nanomaterials with two or more phases of crystalline [35] usually show controllable porous structures and are expected to exhibit excellent performance in water treatments.[19-21]

Magnesium titanate has been investigated to be a promising material as antennas for communication ceramic capacitor resonator radar for its low dielectric loss and high thermal [40] stability at high frequencies.[20] Usually the magnesium titanate consists of two phases, $MgTiO_3$ and $MgTi_2O_5$, and their relevant ratio in the material can be easily adjusted by modulating the synthesis conditions.[23, 24] Recently, the phase mixed magnesium titanate has been demonstrated to be an excellent candidates for [45] photocatalytic hydrogen production.[25] On the other hand, taking into account of the porous structure of the magnesium titanate as well as the well-known specific affinity of Mg and Ti to heavy metal ions, this material is expected also applicable in drinking water treatment as highly efficient absorbents for heavy metal [50] ions.

In this context, porous phase-mixed magnesium titanate nanorods were prepared using a simple ethylene glycol mediated method. Under different Ti/Mg compositions (4/1, 3/1, 1/1, 1/4 and 1/5) and different calcining temperature, the magnesium [55] titanate nanorods were observed to show large difference in various properties, such as surface area crystalline structure and their adsorbing capacity for heavy metal ions.

Experimental section

Synthesis of magnesium titanates

[60] Tetra-n-butyl titanate ($Ti(OC_4H_9)_4$) and magnesium acetate ($Mg(CH_3COO)_2 \cdot 4H_2O$) with varying molar ratio (4/1, 3/1, 1/1, 1/4 and 1/5) were dissolved in 100 mL ethylene glycol (EG) to form clean solutions, respectively, and then the solutions were stirred at room temperature (about 25 °C) for about 12 h and [65] white precursors were obtained. These precursors were washed and centrifuged with absolute ethanol for several times and dried under vacuum at 60 °C overnight. Finally, the precursors were calcined at 500 °C and 600 °C for 2 h in air respectively to obtain the magnesium titanate nanorods. The products were coded as [70] Ti/Mg -A-B, where A represents the molar ratio of initial reactant magnesium acetate and tetra-n-butyl titanate and B represents the calcined temperatures of the precursors, for example Ti/Mg-3/1-500 means the reactant molar ratio of the nanorod is Ti/Mg = 3 and the calcined temperature is 500 °C.

Heavy metal ion adsorption

Lead nitrate were used to prepare solutions with different concentrations of Pb^{2+} ions. The adsorption isotherms were acquired by adding 5 mg magnesium titanates to 30 ml Pb^{2+}

5 solutions (pH=5) of varying concentrations, and stirring overnight at room temperature until adsorption equilibrium. The kinetic behaviors were obtained following the typical steps, 25 mg magnesium titanate nanorods were added into 150 mL heavy metal ions solutions with initial concentration of 20 mg·L^{-1}, and a

10 certain amount of solution was separated and filtered immediately after a specified time, then the solutions were analyzed by inductively coupled plasma−optical emission spectroscopy (Shimadzu ICPE-9000). Recycle tests were carried out using Ti/Mg-3/1-500 as adsorbent and 0.05 mol L^{-1} HCl as desorption

15 solution, respectively. The used adsorbents were mixed with HCl (30 mL) solution and stirred for 12 h. Then the adsorbents were separated from the solution by centrifuging technique. The adsorption and desorption efficiency of the adsorbents were calculated according to the amount of heavy metals in the

20 supernatant.

Characterization

Thermo gravimetric (TG) and differential thermal analysis (DTA) analysis of the samples were conducted on a Pyris 1 TGA unit (Perkin-Elmer USA) in air. The samples were heated to 800

25 °C at the rate of 10 °C·min^{-1}. Shimadzu XRD-7000 diffractometer with Cu K radiation (λ=1.54056 Å) was used to exam crystal structures of the sample. Raman spectra of the samples were obtained using thermo fisher scientific spectrometer at 532 nm. Field emission scanning electron

30 microscope (FE-SEM JEOL JEM 6701F operating at 10 kV) and transmission electron microscopy (TEM JEOL 1011 operating at 100 kV) were adopted to analyze the morphological features of the materials. Nitrogen adsorption/desorption isotherms were performed on a Quantachrome Autosorb AS-1 instrument at 77 K

35 and Barrett–Joyner–Halenda (BJH) model was used to calculate the distribution of the mesopore size.

Result and discussion

Synthesis and characterization of magnesium titanate nanorods.

40 The thermo gravimetric (TG) and differential thermal analysis (DTA) analysis (Fig. 1) together with in-situ XRD (Fig S1) were conducted to select appropriate calcination temperatures to remove organic component of the precursors and crystallize the amorphous nanorods. TG and DTA curves in Fig. 1 reveal that a

45 calcination temperature above 450 °C was required to thoroughly combust organic component of the precursors. Moreover, the samples Ti/Mg-3/1 and Ti/Mg-1/4 show different exothermic peaks indicating that different composition of the materials would influence their crystallization behaviors in the following

50 calcinating process. In-situ XRD analyses in Fig S1 manifest that when the sample was calcined to 700 °C the formed $MgTi_2O_5$ phase began to transform to $MgTiO_3$ phase, suggesting that the heat treating of the samples should be set between 450 and 600°C to maintain two phases of the materials. Therefore, here we

55 calcined the precursors at 500 and 600 °C respectively to obtain magnesium titanate nanorods for further study.
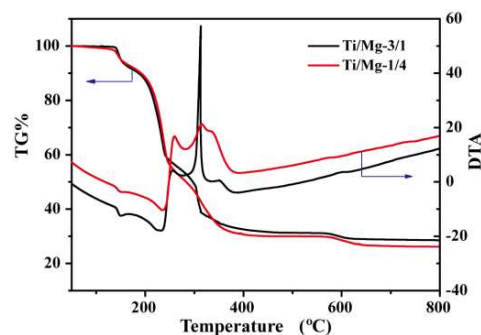

Fig. 1 TG and DTA spectrometry of the two samples Ti/Mg-3/1 and Ti/Mg-1/4.

60 Those magnesium titanates obtained with different molar ratios of Ti/Mg (4/1, 3/1, 1/1, 1/4 and 1/5) have shown different crystallization behaviors, as revealed by X-ray diffraction patterns in Fig. 2. Firstly, the molar ratios of Ti to Mg will influence the crystallization temperature of the samples. As

65 shown in Fig. 2b, when calcined at 500 °C, the nanorod samples Ti/Mg-1/5-500 and Ti/Mg-1/4-500 are in amorphous form and the samples start to crystallize only while the molar ratio of Ti/Mg > 1. Moreover, the sample crystallinity enhances quickly along with the Ti/Mg ratio increasing. This suggests that the

70 samples tend to crystalize at lower temperature with higher Ti/Mg molar ratios. Additionally, the molar ratios of Ti/Mg also affect the crystalline phase of the nanorods. As shown in Fig. 2a, while the samples with molar ratios of Ti/Mg > 1 were calcined under 600 °C, the primary crystalline phase of the nanorods was

75 $MgTi_2O_5$ with base-centered orthorhombic structure (JCPDS no. 35-0792). Along with the Ti/Mg ratio increasing the amount of the $MgTi_2O_5$ phase increased and finally pure $MgTi_2O_5$ phase was observed at Ti/Mg = 4/1, as shown in Fig. 2a and Fig. S2. When decreasing the molar ratio of Ti to Mg less than 1, phase-

80 mixed nanorods containing $MgTi_2O_5$ and $MgTiO_3$ were obtained and the amount of $MgTiO_3$ with rhombohedral structure (JCPDS no. 06-0494) increased and turned to be the prime phase of the nanorods, as shown in Fig. 2a and Fig. S2.
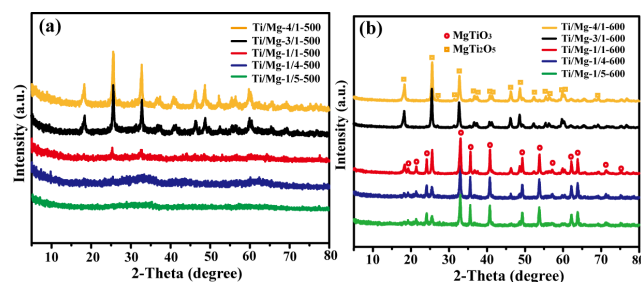

85 Fig. 2 XRD patterns of the precursors calcined at (a) 500 °C and (b) 600 °C.

Besides their crystallization behaviors, the morphologies of the magnesium titanate nanorods with different Ti/Mg molar ratios calcined at 500 and 600 °C were also investigated by TEM and

90 SEM images respectively, as shown in Fig. 3, and the variation trendency are shown in Scheme 1. Under 500 °C heating treatment and the molar ratios of Ti/Mg < 1，it was observed that

the nanorods show bubble-like porosities (Fig.3d and e), suggesting a high surface area of the materials. However, along with the Ti/Mg ratio increasing (Ti/Mg >= 1), small crystal particles began to appear in the nanorods, and worm-like
5 porosities were found to form due to the consumption of organic component in the precursors (Fig. 3a b and c), which is well in accord with the XRD results displayed in Fig. 2b. While the samples calcined at 600 °C, as shown in Fig. 3f-j, the crystalline nanorods displayed evidently enlarged pore network and coarse
10 surface. Moreover, the size of constituent particles in the nanorods increased along with the decreasing of Ti/Mg molar ratios, which can be attributed to the bubble-like porosities that provide more space inside the nanorods for the crystal growth. Fig 3k-o show low magnified SEM images of the samples under
15 the same conditions and it was observed that the nanorods with higher Ti/Mg molar ratio show larger length-diameter ratio smaller constituent particles and hence smoother surface. The change trends of the morphology and grain size of the nanorods with differernt Ti to Mg molar ratios are shown in Scheme 1.
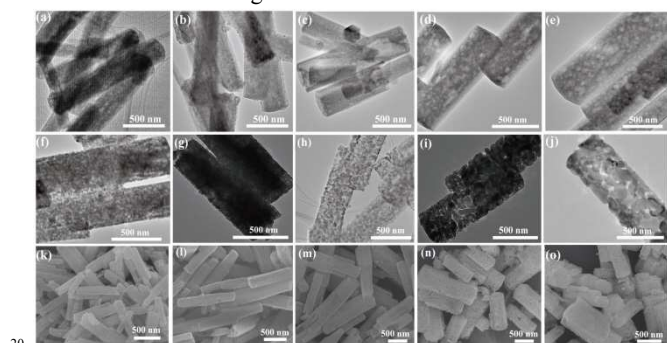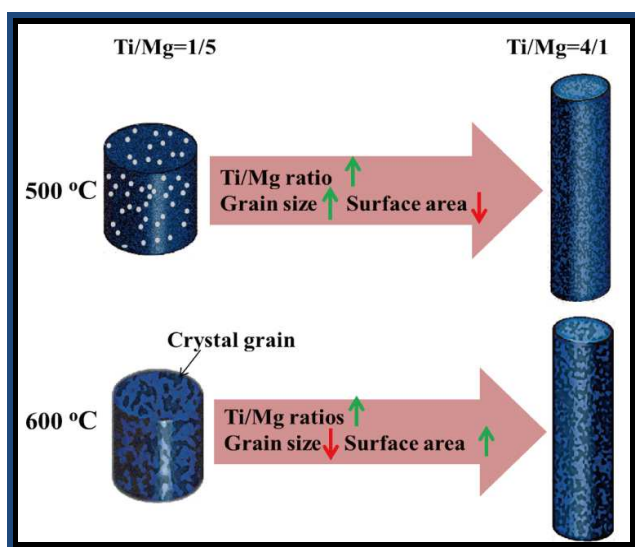

20 Fig. 3 TEM images of nanorods calcined at (a-e) 500 °C and (f-j) 600 °C with Ti to Mg molar ratios of 4/1, 3/1, 1/1, 1/4 and 1/5, respectively; (k-o) SEM images of nanorods calcined at 600 °C with Ti to Mg molar ratios of 4/1, 3/1, 1/1, 1/4 and 1/5,
25 respectively.

Scheme 1. Grain size and surface areas changing trend of the nanorods with different Ti/Mg ratios calcined at 500 °C and 600 °C, respectively.

30 Diffusion and adsorption properties of an adsorbent are often influenced by its porosity and surface area. N_2 adsorption–

desorption analysis therefore was proformed to characterize the porosity of the nanorods. Representative sorption isotherms and pore size distribution profiles obtained for the Ti/Mg-4/1, Ti/Mg-
35 1/1 and Ti/Mg-1/5 samples calcined at different temperatures were shown in Fig. 4. Sorption isotherms in Fig. 4 showed that the Ti/Mg-500 nanorods exhibited higher surface areas than those of Ti/Mg-600 nanorods. Moreover, the pore size distribution profiles shown in Fig. S3 revealed a notable mesopore size
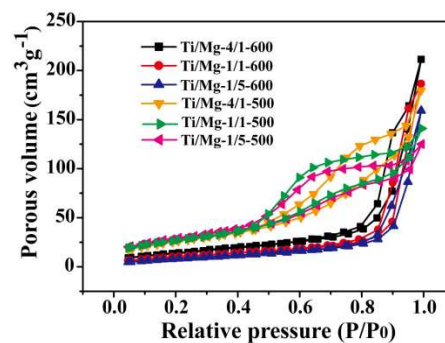40 enlargement from ca. 3−12 nm for Ti/Mg-500 to ca. 10−30 nm for Ti/Mg-600 system.

Fig. 4 Representative nitrogen adsorption/desorption isotherms of the nanorods.

45 The formation of porous structure of Ti/Mg-500 and Ti/Mg-600 system is mainly attributed to the removal of organic molecules while heating treatment of the materials, as observed from the TEM images (Fig 3a-j). Obviously, the chemical composition of the materials plays a key role in determining the crystalline and
50 morphological structure of the nanorods, so the changing of Ti/Mg molar ratios and the annealing temperature would lead to different porous structure of the magnesium titanate. Fascinatingly, as revealed in Table 1, the pore size of the nanorods for Ti/Mg-500 system increased while enhancing the
55 Ti/Mg molar ratios, but contrary trend was observed in Ti/Mg-600 system. This behavior may be assigned to the different crystalline size of the magnesium titanate under different annealing temperature. For example, the higher crystallinity and larger pore size of Ti/Mg-4/1-500 contribute to its lower surface
60 area in Ti/Mg-500 system, while in Ti/Mg-600 system, Ti/Mg-4/1-600 showed highest surface area due to its smallest grain and pore size, and this agreed well with the TEM results in Fig. 3.

Heavy Metal Ion adsorption studies

Pd(II) is one of the most common and toxic aqueous heavy
65 metal cation ions and its efficient removal is vital for drinking water safety. The representative adsorption rates of magnesium titanate nanorods Ti/Mg-500 and Ti/Mg-600 for Pb^{2+} were shown in Fig.5a. The magnesium titanate nanorods have a steep uptake of the heavy metal ions in the beginning and a plateau reached
70 soon after 10 minutes, which indicates the strong binding interactions between the lead ions and magnesium titanate nanorods. It was observed that the adsorption equilibrium was achieved within 1 h, indicating the very fast adsorption processes of the absorbents.
75 The effect of different Ti/Mg ratios and crystallinity of the magnesium titanate nanorods on their sorption properties of Pb^{2+} was investigated by monitoring the adsorption of lead ions at varying initial concentrations of 10−80 ppm. Langmuir model

was used to analyze the adsorption process according to equation:[17] $q_e = q_m(bc_e)/(1+bc_e)$, where q_e (mg·g^{-1}) is the equilibrium adsorption capacities of the heavy-metal ions; q_m (mg·g^{-1}) is the maximum adsorption capacity of the heavy-metal ions; C_e (mg·L^{-1}) is the equilibrium concentration of the ions in the testing solutions and b (L·mg^{-1}) is the equilibrium constant.

The steep uptakes of the heavy metal ions at lower solute concentrations and a plateau reached with increasing in equilibrium solute concentration suggested the monolayer coverage of lead ions on the adsorbents surface, the characteristic of Langmuir adsorption behavior. All the experimental data fits the Langmuir adsorption isotherm well (Fig. 5b, c) and the R^2 along with b values and maximum adsorption capacity (q_m) of the as-prepared magnesium titanate nanorods are summarized in Table 1. It can be found that the adsorption capacities of the nanorods were proportion to their surface areas. As shown in Fig. 5b, the adsorption isotherms of the nanorods calcined at 500 °C can be divided to two groups, i.e. the nanorods with amorphous or semi-crystal and crystal structures. Obviously, the amorphous structure of magnesium titanate nanorods owned higher surface area than the crystalline group, leading to much higher adsorption capacity for Pd(II).
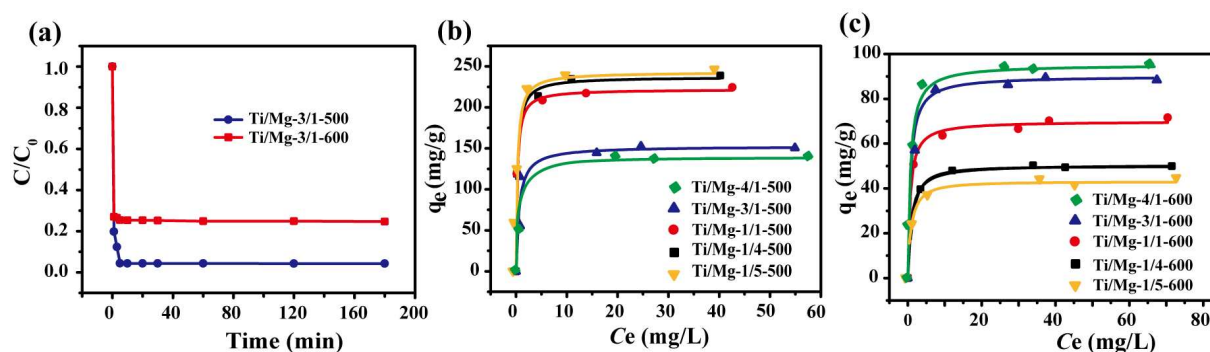

Fig. 5 (a) Adsorption rates curves of Pb^{2+}, the initial ion concentration is 20 mg·L^{-1} and sample dose is 25 mg/150 mL. Adsorption isotherms of Pb^{2+} with (b) Ti/Mg-500 system and (c) Ti/Mg-600 system as adsorbents, the initial ion concentration is 10~80 mg·L^{-1} and sample dose is 5 mg/30 mL.

Table 1. Properties of magnesium titanate nanorods and their adsorption capacities for Pd(II).

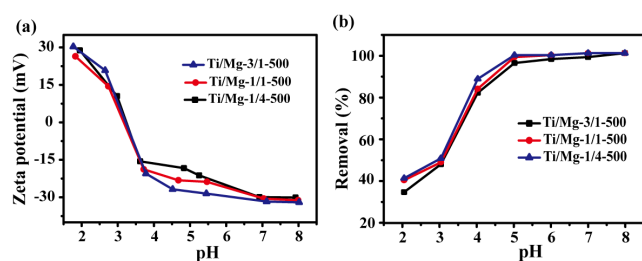|	R^2	b(L·m^{-1})	q_m(mg·g^{-1})	Surface area (m^2·g^{-1})	Pore size (nm)
Ti/Mg-4/1-500	0.917	1.58	143	103.2	3-12
Ti/Mg-3/1-500	0.912	1.63	153	106.4	3-12
Ti/Mg-1/1-500	0.946	3.9	222	138.4	3-8
Ti/Mg-1/4-500	0.961	3.4	237	149.6	3-8
Ti/Mg-1/5-500	0.953	3.6	241	152	3-8
Ti/Mg-4/1-600	0.997	1.43	106	66.2	10-30
Ti/Mg-3/1-600	0.998	1.49	91	55.11	10-30
Ti/Mg-1/1-600	0.994	1.62	70	38.36	10-30
Ti/Mg-1/4-600	0.997	1.08	51	33.5	10-30
Ti/Mg-1/5-600	0.998	1.03	44	28.5	10-30

Fig. 6 (a) zeta potentials and (b) removal efficiency of the

representative nanorods of Ti/Mg-500 system with varying pH values.

Besides of surface area, surface charge property was also a vital factor that affects the adsorption capacity of an adsorbent. Thus zeta potentials of the three representative nanorods (Ti/Mg-3/1-500, Ti/Mg-1/1-500 and Ti/Mg-1/4-500) with varying pH of their solutions were further studied. As shown in Fig. 6a, the PZC of all the three nanorods were about 3.25, which indicated their surfaces were highly negatively charged. Such negatively charged

surface of the nanorods not only attract Pb^{2+} through electrostatic interactions but also prevent the absorbents aggregation in solution, which is beneficial to the heavy metal cations removal. Moreover, the Pb^{2+} adsorption performance of magnesium titanate nanorods was examined under different pH values, as presented in Fig. 6b, it was revealed that the nanorods possess outstanding adsorption capacity over a wide range of pH values. It is an important step to regenerate the adsorbent to make the adsorption process more economical. As shown in Fig. S4, the adsorbent maintained its adsorption/desorption efficiencies for Pb (II) after 3 cycles of repeated adsorption and desorption., suggesting that the adsorbent can be recycled. Moreover, the SEM image and XRD pattern of the used adsorbent (Fig. S5) was similar to that of the fresh sample, demonstrating the good stability and reusability of the adsorbent.

Conclusions

In summary, magnesium titanate nanorods with different Ti/Mg ratio have been prepared via a simple ethylene glycol-mediated route. The chemical compositions of the nanorods have shown significant impact on their properties, such as crystallinity, morphology, surface areas and pore structures. The adsorption performances of the magnesium titanate nanorods with changed chemical compositions have been studied.The adsorption of Pb^{2+} onto the adsorbents was confirmed to be an electrostatic interaction process and the removal capacities were positively relate to their surface areas.

Acknowledgements

Notes and references

aLaboratory of Molecular Nanostructure and Nanotechnology, Institute of Chemistry, Chinese Academy of Sciences, Beijing 100190, China.jiangli@iccas.ac.cn, crwang@iccas.ac.cn.

bUniversity of the Chinese Academy of Sciences, Beijing 100049 China.

1 J. O. Nriagu, J. M. Pacyna, Nature, 1988, 333, 134-139.

2 I.-H. Chang, J. J. Tulock, J. Liu, W.-S. Kim, D. M. Cannon, Y. Lu, P. W. Bohn, J. V. Sweedler, D. M. Cropek, Environ. Sci. Technol.,2005, 39, 3756-3761.

3 H. Hu, Q. Jin, P. Kavan, Sustainability-Basel, 2014, 6, 5820-5838.

4 A. K. Jorgenson, Int. Sociol., 2009, 24, 115-143.

5 B. Wang, H. Wu, L. Yu, R. Xu, T. T. Lim, Adv. Mater., 2012, 24, 1111-1116.

6 X. Yang, X. Wang, Y. Feng, G. Zhang, T. Wang, W. Song, C. Shu, L. Jiang, C. Wang, J. Mater. Chem. A, 2013, 1, 473-477.

7 W. Liu, F. Huang, Y. Wang, T. Zou, J. Zheng and Z. Lin, Environ. Sci. Technol., 2011, 45, 1955-1961.

8 W. Liu, F. Huang, Y. Liao, J. Zhang, G. Ren, Z. Zhuang, J. Zhen, Z. Lin and C. Wang, Angew. Chem. Int. Ed., 2008, 47, 5619-5622.

9 Z. Ma, D. Zhao, Y. Chang, S. Xing, Y. Wu and Y. Gao, Dalton Trans.,2013, 42, 14261-14267.

10 X.-Y. Yu, R.-X. Xu, C. Gao, T. Luo, Y. Jia, J.-H. Liu and X.-J. Huang, ACS Appl. Mater. Interfaces, 2012, 4, 1954-1962.

11 C.-Y. Cao, J. Qu, F. Wei, H. Liu and W.-G. Song, ACS Appl. Mater. Interfaces, 2012, 4, 4283-4287.

12 R. S. Azarudeen, R. Subha, D. Jeyakumar and A. R. Burkanudeen, Sep. Purif. Technol., 2013, 116, 366-377.

13 X. Wei, X. Kong, S. Wang, H. Xiang, J. Wang and J. Chen, Ind. Eng. Chem. Res., 2013, 52, 17583-17590.

14 L. Wu, L. Liao, G. Lv, F. Qin, Y. He and X. Wang, J. Hazard. Mater., 2013, 254, 277-283.

15 X. Wang, X. Yang, J. Cai, T. Miao, L. Li, G. Li, D. Deng, L. Jiang and C. Wang, J. Mater. Chem. A, 2014, 2, 6718-6722.

16 J. Qu, W. Li, C.-Y. Cao, X.-J. Yin, L. Zhao, J. Bai, Z. Qin and W.-G. Song, J. Mater. Chem., 2012, 22, 17222-17226.

17 J. Qu, C.-Y. Cao, Y.-L. Hong, C.-Q. Chen, P.-P. Zhu, W.-G. Song and Z.-Y. Wu, J. Mater. Chem., 2012, 22, 3562-3567.

18 X. M. Zhang, J. Y. Liu, S. J. Kelly, X. J. Huang and J. H. Liu, J. Mater. Chem.A, 2014, 2, 17759-11767.

19 D. Chen, L. Cao, T. L. Hanley and R. A. Caruso, Adv. Funct. Mater., 2012, 22, 1966-1971.

20 M. Chee Kimling, N. Scales, T. L. Hanley and R. A. Caruso, Environ. Sci. Technol., 2012, 46, 7913-7920.

21 G. L. Drisko, V. Luca, E. Sizgek, N. Scales and R. A. Caruso, Langmuir, 2009, 25, 5286-5293.

22 C.-L. Huang, C.-H. Shen and T.-C. Lin, J. Alloy. Compd., 2009, 468, 516-521.

23 H. Kang, L. Wang, D. Xue, K. Li and C. Liu, J. Alloy. Compd., 2008, 460, 160-163.

24 Y.-M. Miao, Q.-L. Zhang, H. Yang and H.-P. Wang, Mater. Sci. Eng. B, 2006, 128, 103-106.

25 Y. Qu, W. Zhou, Y. Xie, L. Jiang, J. Wang, G. Tian, Z. Ren, C. Tian and H. Fu, Chem. Commun., 2013, 49, 8510-8512

Ti/Mg molar ratios will influence the properties of the magnesium titanate nanorods, such as morphology, surface area, crystallinity and crystal structure, and then their adsorption capacities for Pb^{2+} .